Tribology Letters (2018) 66:47
https://doi.org/10.1007/s11249-018-0994-1

ORIGINAL PAPER

Friction and Wear Characteristics of Single Crystal Ni-Based Superalloys at Elevated Temperatures

Pantcho Stoyanov[1] · Lesley Dawag[1] · Daniel G. Goberman[2] · Dilip Shah[1]

Received: 11 August 2017 / Accepted: 29 January 2018

Abstract
The purpose of this study was to investigate the friction and wear behavior of single crystal superalloys at elevated temperatures. Pin-on-plate experiments were conducted using a custom-built high-temperature fretting/wear apparatus. Measurements were performed on two single crystal Ni-based alloys and Waspaloy® (used as a baseline material). The coefficient of friction for the single crystal materials (i.e., during running-in and steady state) was lower compared to the Waspaloy®. In addition, the experiments showed that the friction coefficient of the single crystal is dependent on the crystallographic plane; the friction coefficient was lower for the tests on the {100} plane compared to the {111} plane. The wear behavior was aligned with the friction behavior, where the single crystal Ni-based alloys showed slightly higher wear resistance compared to the Waspaloy®. Ex situ analysis by means of FIB/SEM and XPS analysis revealed the formation of Co-base metal oxide layer on the surface of the single crystal alloy. Similarly, a Co-base oxide layer is observed on the counterface providing a self-mated oxide-on-oxide contact and thus lower friction and wear compared to the Waspaloy®.

Keywords Single crystal alloys · Tribofilm · Lubricious oxides

1 Introduction

Nickel-based superalloys are widely used as structural components in demanding environments due to their excellent stability (i.e., resistance to mechanical and chemical degradation) at elevated temperatures [1–10]. These superalloys were primarily developed to meet the demand of jet engine and industrial gas turbine engine blades operating at temperature in excess of 980 °C [1, 6, 11]. Such alloys consist of nickel-based solid solution, referred to as γ-matrix with a dispersion of precipitates, generally referred to as γ′. The precipitates are hard intermetallic Ni_3(Al, X) compounds, where X is typically Ti, Nb or Ta. The γ-matrix (i.e., FCC crystal structure) is largely coherent with the γ′ precipitates (i.e., $L1_2$ crystal structure), which allows the precipitation-hardened microstructure to remain very stable at high temperatures [1, 6]. This is one of the primary reasons such alloys have been very successful for high-temperature application. The early generation of such alloys contained about 40% by volume of the precipitate, and the most commonly used Waspaloy® is a typical example of that. However, with increasing temperature demand, it was realized that alloys with 65% precipitate by volume were optimum for achieving a balance of high-temperature creep resistance and tensile strength [1, 6]. The early generation of such alloys was polycrystalline and typically used in cast form using investment casting techniques to achieve complex shapes. Subsequently, it was recognized that creep resistance of such alloys can be further improved by eliminating the grain boundaries (i.e., high diffusion paths) normal to the principal stress. Consequently, this led to the development of directional solidification of columnar grain alloys and eventually single grain or single crystal castings [1, 10]. The development of single crystal technology by Pratt & Whitney allowed addition of refractory alloying elements as Ta and Re with further improvement in temperature performance. More details on various aspects of superalloys can be found elsewhere [1].

The precipitate microstructure can be naturally formed using a series of heat treatments, and thus, an optimum balance of mechanical properties can be achieved by judiciously varying the heat treatment sequence. It is a common

✉ Pantcho Stoyanov
pantcho.stoyanov@pw.utc.com

[1] Pratt & Whitney, United Technologies Corporation, East Hartford, CT, USA

[2] United Technology Research Center, United Technologies Corporation, East Hartford, CT, USA

Published online: 10 February 2018

metallurgical principle that finer precipitate structure results in harder material and coarser precipitate structure results in softer material. For most applications, superalloys are used with the precipitate size ranging from 0.3 to 0.5μm. However, if softer material is desired then the alloy may be overaged to achieve precipitate size approaching 1μm. This extreme case is referred to as the super-overaged (SOA) condition.

Unfortunately, while intensive alloy and process development activities for these high-temperature superalloys have been performed over the last few decades, their tribological behavior (i.e., friction and wear) has received little attention [12, 13]. With the increasing demand in temperature and spread of application of these alloys to other static and dynamic components in the engine, there is a clear need for a better understanding of their tribological behavior. However, understanding the friction and wear behavior at high temperatures of metallic alloys is much more challenging compared to their behavior at room temperature [13]. Indeed, as suggested by Blau [13], the wear behavior of metallic alloys at elevated temperatures can vary depending on the contact conditions and nature of the oxide layer formation. Thus, several research efforts have been performed in order to study the tribofilm (i.e., oxide layers) formation of wear-resistant alloys such as Co-based and Ni-based alloys at elevated temperatures [14–16]. For instance, Scharf et al. [14] showed that the formation of a Co-based oxide 'glaze' layer in Haynes 25 alloys resulted in lower friction and wear. Similarly, Scott et al. [15] identified the formation of a glaze layer of Stellite 31 above 523 K under their sliding conditions.

Fewer studies have been performed on the friction and wear behavior of Ni-based superalloy single crystals at high temperatures. In a study on wear resistance of tribocouples at elevated temperatures, Lawen et al. [16] provided results of friction and wear behavior in single crystal Ni alloy. However, the underlying mechanisms of Ni-based single crystal alloys leading to low friction and wear at elevated temperature remain unclear. This paper is a first and modest attempt to close this gap in a systematic way.

The major objectives of this study were to (1) evaluate the friction and wear performance of single crystal Ni-based alloys at elevated temperatures and (2) determine the interfacial mechanisms governing the friction and wear behavior, including oxide formation and microstructural changes.

2 Experimental Procedure

Pin-on-plate experiments were conducted using custom-built high-temperature fretting/wear apparatus. Briefly, a load cell located on the upper and lower portion of the rig was used to measure the friction force, while a static normal load was applied and measured using load cells. A servo-hydraulically driven actuator controlled the displacement and frequency of the plate relative to the stationary pin. The tests were performed at elevated temperature of 790 °C using normal stresses of 5.87 MPa, a frequency of 0.25 Hz and a displacement of 4.27 mm for 2000 cycles. The relative humidity in the laboratory was approximately 45% RH. These parameters were chosen based on equipment capability and typical fretting conditions for these alloys. Hardness was measured using a Rockwell hardness tester (United, True-Blue II) on the unworn surface of the tested specimen (i.e., after exposure to the elevated temperature). The hardness results are presented as an average from five measurements each.

Materials used for plates were two Ni-based single crystal superalloys with a nominal chemistry provided in Table 1 [1]. Waspaloy® served as a baseline. The single crystal material was either conventionally heat-treated (CHT) or overaged to produce coarse γ′ (SOA). The SOA single crystal materials were heat-treated to obtain precipitate size approaching 1 μm. Typical heat treatment conditions and procedure for the single crystal alloys can be found elsewhere [1]. The pin for each experiment was CHT PWA1484. This material was chosen as the pin to represent typical counterface materials in the high-temperature region of the engine. In addition, experiments on PWA1484 were performed on the {100} and the {111} crystallographic faces. These samples were machined accordingly to obtain the desired surface orientation, which was verified by means of Laue diffraction.

X-ray photoelectron spectroscopy (XPS) (PHI VersaProbe, Physical Electronics Inc.) analysis was performed on the worn and unworn surfaces (i.e., after testing/exposure to elevated temperature) in order to provide a better understanding of the chemical changes. This analysis was represented in terms of the sputtering depth. Based on depth calibrations with 1000 Å Ta_2O_5 on Ta, a sputtering time of 10 min can be estimated to be approximately 60 nm. Prior to the analysis, the samples are cleaned using isopropanol followed by cyclohexane. These data provided high binding

Table 1 Typical compositions of the alloys tested [1]

	Cr	Co	Mo	W	Al	Ti	Ta	Re	Hf	C	B	Ni
PWA1484	5.0	10.0	2.0	6.0	5.6	–	9.0	3.0	0.1	–	–	Bal
PWA1480	10.0	5.0	–	4.0	5.0	1.5	12.0	–	–	–	–	Bal
Waspaloy®	19.5	13.5	4.3	–	1.3	3.0	–	–	–	0.8	0.006	Bal

energy resolution and high depth resolution offering elemental concentration information from the surface down to ~ 220 nm below the surface. Focused ion beam scanning electron microscopy (FIB/SEM) (FEI Helios 600 NanoLab DualBeam FIB) was used to cut site-specific cross sections of two of the surfaces (i.e., in the worn and unworn state after testing/heat exposure), and images/elemental maps of those locations were acquired. While utilization of the EDS offered lower resolution elemental distribution information than the XPS, the information covered a much larger depth, from the surface down to ~ 10 µm into the worn surface.

3 Results and Discussion

3.1 Friction and Wear

The friction behavior as a function of sliding cycles is shown in Fig. 1 for the various surfaces tested at 790 °C. The coefficient of friction is evidently higher for the Waspaloy® compared to that of the single crystal materials. The lowest coefficient of friction is observed with PWA1484 {100} in the SOA condition up to approximately 1500 cycles. Subsequently, the friction is similar for PWA1480 and PWA1484 SOA. Interestingly, the {111} plane showed slightly higher friction compared to the {100} plane of the single crystal PWA1484. It should also be noted that while all materials experience a running-in period, steady-state sliding is obtained quicker (i.e., fewer cycles) with the Waspaloy® compared to the single crystals.

The wear behavior of the Ni-based superalloys is shown in Fig. 2. Similarly to the coefficient of friction, the wear of the Waspaloy® is higher compared to the one of the single crystal PWA1484 CHT and PWA1480. However, the PWA1484 SOA showed the most wear compared to all other materials, which is opposite to the friction behavior. The wear results showed a reverse correlation to the hardness of the materials, as shown in Fig. 2. The lowest hardness

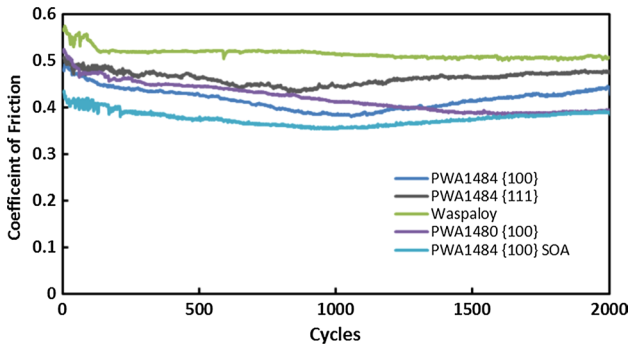

Fig. 1 Average coefficient of friction versus sliding cycles for the single crystal Ni-based alloys and Waspaloy® tested at 790 °C

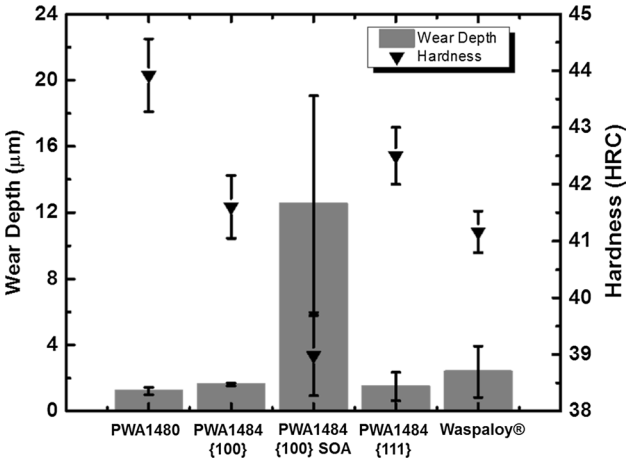

Fig. 2 Average wear depth and hardness for the single crystal Ni-based alloys and Waspaloy® tested at 790 °C

is observed with PWA1484 SOA, and the hardness of the Waspaloy® was slightly lower compared to the other single crystal materials (i.e., PWA1484 and PWA1480). It should be noted that for all experiment transfer of material was observed on the single crystal counterface.

3.2 Ex Situ Analysis

Cross-sectional SEM images are shown in Fig. 3 for both, the worn and unworn surfaces of the single crystal and Waspaloy®. The micrograph of the unworn surface (Fig. 3a, b) shows slight microstructural changes in the near-surface region, which have likely been caused by the sample cutting process. In addition, the oxidation behavior of the unworn surfaces was different between the Waspaloy® and PWA1484. The elemental mapping of the Waspaloy® revealed the formation of a ~ 0.7-µm-thick chromium oxide layer on the surface and an aluminum oxide layer beneath. The micrograph of the single crystal alloy on the other hand only showed a thin aluminum oxide layer (i.e., 0.1–0.2 µm). The chromium oxide layer was not observed on the single crystal alloy. Consequently, the friction-induced changes to the chemistry were different compared for the two alloys (i.e., Waspaloy® and single crystal PWA1484). Figure 3c clearly shows the formation of a Co-rich oxide layer on the surface of the single crystal PWA1484. In addition, the elemental mapping showed high molybdenum content near the surface in most regions. It should be noted that oxidized nickel was also present in some regions of the subsurface. However, aluminum or chromium was not detected near the surface. In comparison, the chromium and aluminum oxide layer was still present in most regions of the worn Waspaloy® surface, as shown in Fig. 3d. Small amount of nickel and molybdenum was also present near the surface of the Waspaloy®.

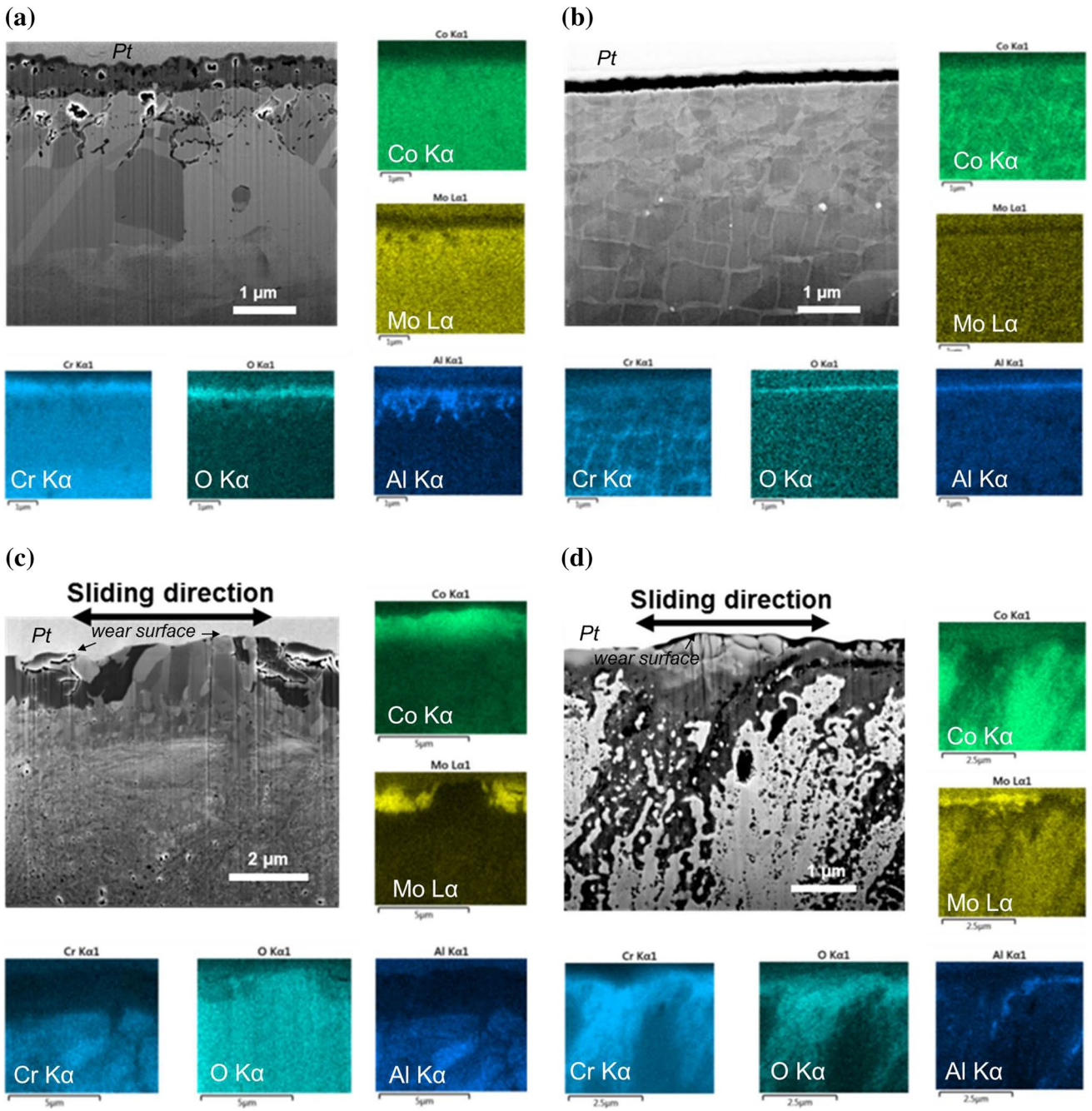

Fig. 3 Cross-sectional SEM images produced by FIB of **a** the unworn single crystal PWA1484 CHT {100}, **b** the unworn Waspaloy®, **c** the worn single crystal PWA1484 {100} parallel to the sliding direction and **d** the worn Waspaloy® parallel to the sliding direction

XPS was performed in order to further elucidate the friction-induced chemical changes within a few nanometers from the worn surface. The XPS depth profiles of the wear tracks and the unworn surfaces are shown in Fig. 4. Similarly to the cross-sectional SEM images, higher cobalt content was observed near the surface of the single crystal PWA1484 {100} compared to the Waspaloy®. The cobalt was mainly in form of oxide throughout the depth confirming the observation of the SEM images. Small amount of oxidized molybdenum ($\leq$ 5 at.%) was also observed on the single crystal PWA1484 {100} and the Waspaloy®. The nickel content (i.e., mostly in the form of oxide) near the worn surface of the crystal was higher compared to the Waspaloy®, while the chromium oxide content was higher in the Waspaloy®. This was consistent with the XPS analysis of the unworn surfaces, where a

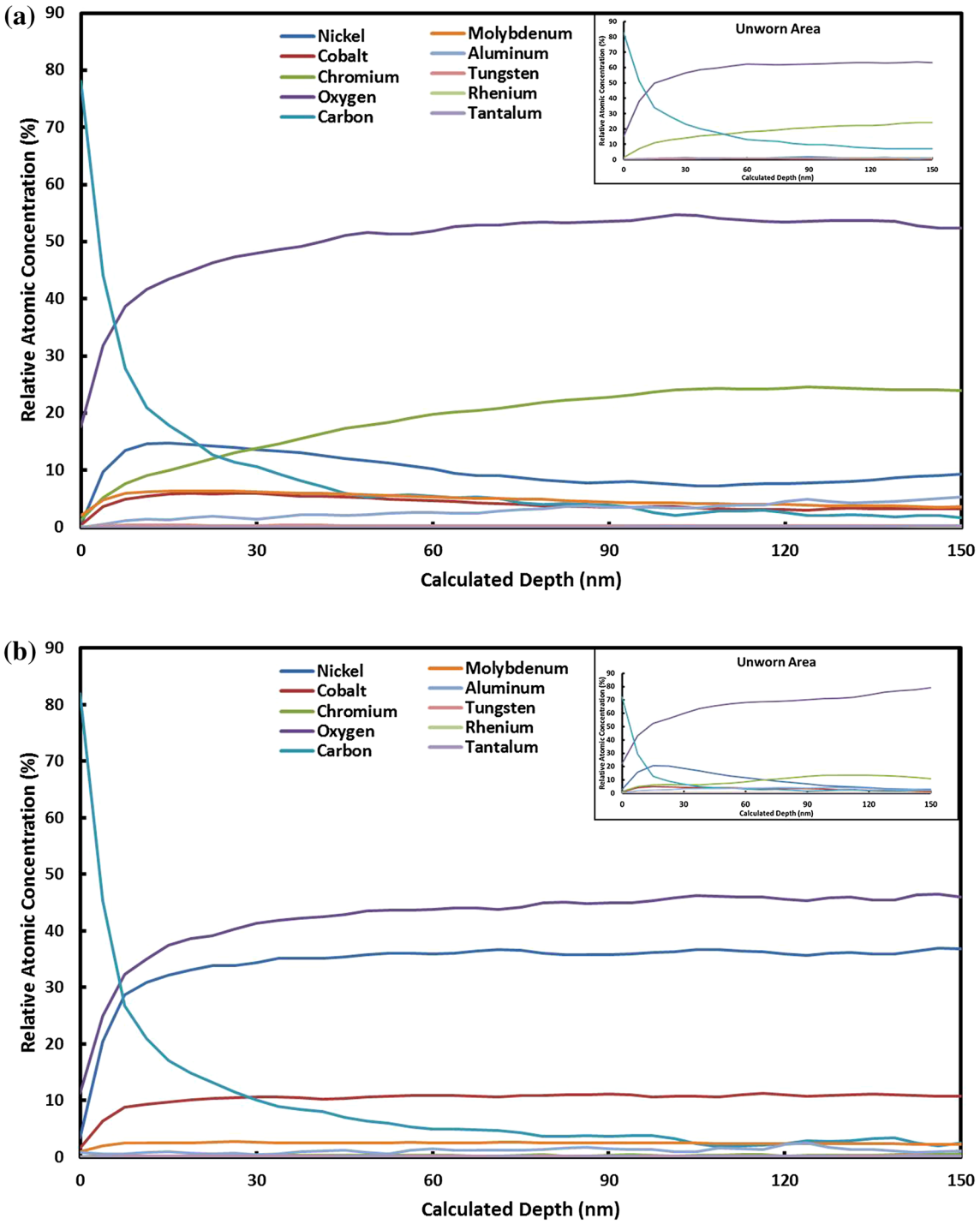

Fig. 4 XPS depth profile on the worn surface of **a** the Waspaloy®, **b** the single crystal PWA1484 CHT {100} and **c** the single crystal PWA1484 CHT {111}. The inserts in the figures show the depth profile of an unworn area as a comparison

thick chromium oxide layer is present in the unworn state of the Waspaloy®.

Interestingly, the XPS profile of the PWA1484 {111} was slightly different compared to the {100} surface; the cobalt content was lower in the {111}, and no molybdenum oxide was present near the surface (< 50 nm from the surface). In addition, the chromium concentration was also higher with the {111} crystal surface compared to the {100}. This is also consistent with the unworn state, where higher chromium and lower cobalt and molybdenum oxides are observed with the {111} unworn surface.

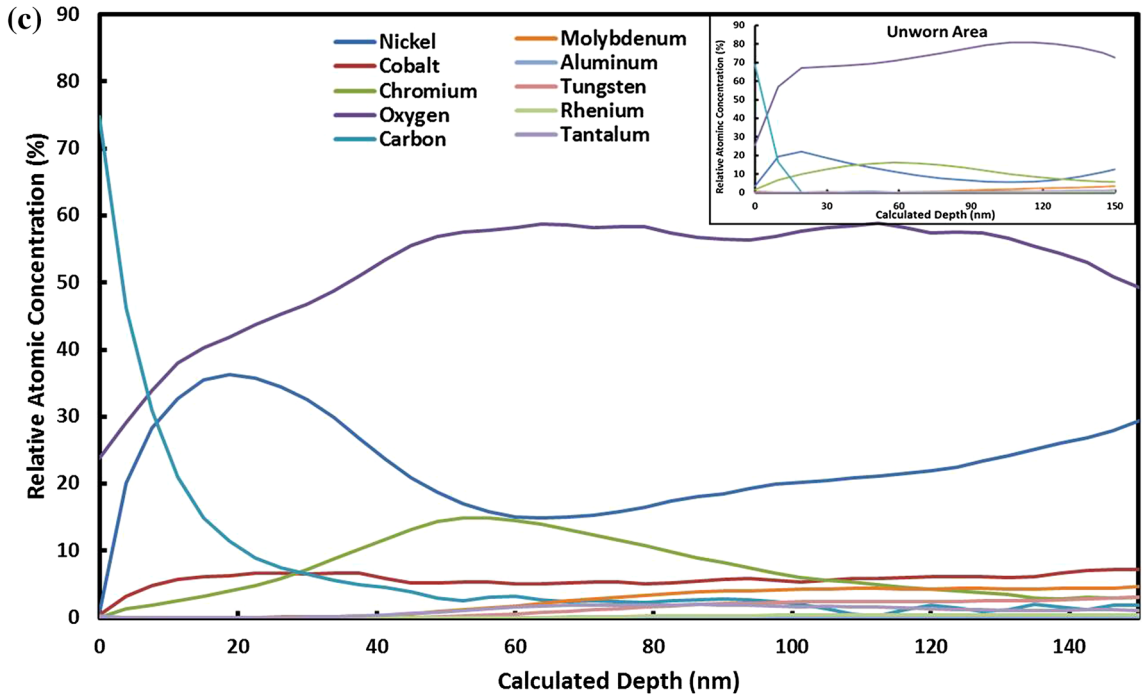

Fig. 4 (continued)

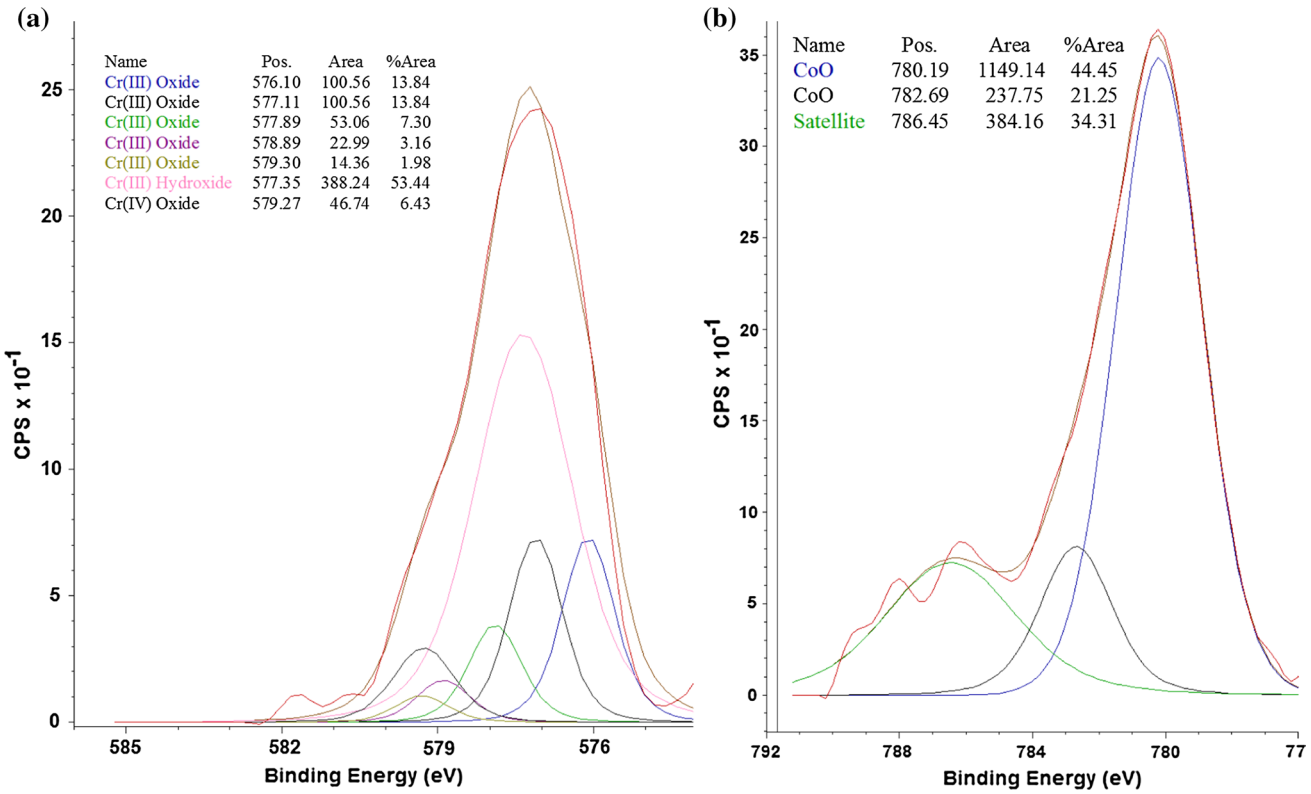

Fig. 5 XPS analysis of **a** the Waspaloy®, **b** the single crystal PWA1484 CHT {100}

In order to provide a better understanding of the oxide behavior, Fig. 5 shows the Cr and Co peak fitting of the worn Waspaloy and PWA1484, respectively. Cr 2*p*3/2 peak fitting in the Waspaloy sample reveals a complex oxide state with Cr(III) oxide and hydroxide dominating the surface chemical state (see Fig. 5a). Small amount of Cr(IV) oxide is also observed [17]. Co 2*p*3/2 peak fitting in the PWA1484 samples, on the other hand, indicates a CoO oxide state as dominant at the surface [17], though contributions from both Co and Ni Auger peaks affect the theoretical peak intensities.

Figure 6 shows the corresponding XPS depth profiles of the single crystal PWA1484 counterfaces used on the Waspaloy® and the single crystal PWA1484. Similarly to the analysis on the wear tracks, the cobalt content (i.e., oxidized) was higher for the single crystal PWA1484 {100} compared to the Waspaloy®. The cobalt content in the PWA1484 {111} was also lower compared to the {100} crystal surface.

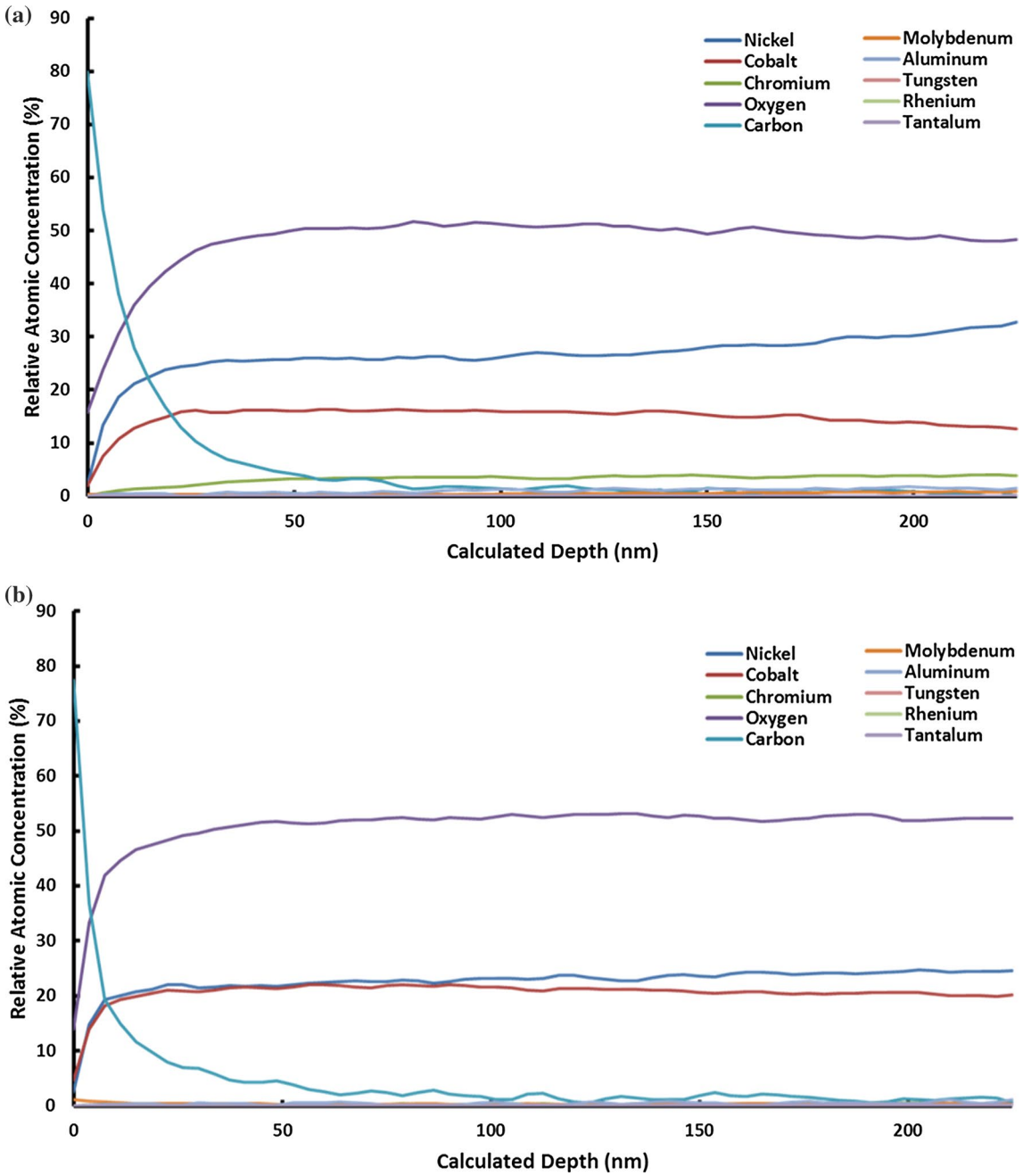

Fig. 6 XPS depth profile on the worn surface of **a** the Waspaloy®, **b** the single crystal PWA1484 CHT {100} and **c** the single crystal PWA1484 CHT {111}

The chemical analysis indicated the formation of cobalt-based oxide layer on the single crystal PWA1484 surface. Similarly, a cobalt-based oxide layer was observed on the counterface indicating self-mated oxide-on-oxide sliding. Thus, the lower friction with the PWA1484 is attributed to the formation of the Co-based oxide layers on both sliding surfaces. The analysis of the Waspaloy®, on the other hand, did not reveal a Co-based oxide layer on the worn surface. This can possibly be explained by the higher chromium content in the Waspaloy® leading to the formation of a relatively thick Cr-rich oxide layer at elevated temperatures in the unworn state. Consequently, the presence of this Cr-rich oxide layer on the unworn Waspaloy® surface limits the possibility of the Co-based oxide layer formation during sliding and thus results in higher friction and wear. Lower friction coefficient with cobalt oxides compared to chromium oxides has been previously reported at elevated temperatures (i.e., ~ 700 °C) and is attributed to formation of continuous solid films rather than being brushed away by the sliding [18].

Interestingly, the {111} crystallographic plane of the single crystal exhibited slightly higher friction and wear compared to the {100} plane. Consistently, the XPS analysis showed higher Cr oxide content and no evidence of Mo oxide near the worn surface. In addition, their oxide layer formation in the unworn state at 790 °C is slightly different, where the {111} crystallographic plane had lower Mo and Co content with slightly higher Cr oxide. It should be noted that the different surface orientation could potentially result in different surface energy, elastic moduli as well as plastic deformation [1], which could have possibly contributed to the different friction values. However, this phenomenon will be investigated in more detail and presented in a future study.

Formation of self-mated oxide-on-oxide glaze at the sliding interface has been previously observed with Haynes 25 cobalt-based superalloy sliding against Ta–W alloy [14]. The authors identified the oxide layer as predominantly (Co, Cr) O, by means of FIB-SEM and TEM. Interestingly, the oxide glaze layer only formed when testing at elevated temperatures (i.e., 430 °C) in conjunction with the low friction and wear. Consistently, Viat et al. performed a series of studies on the glaze layer formation of Haynes 25 [19–21] and showed the formation of a glaze layer, which adhered to both counterparts (i.e., Haynes 25 and ceramic counterface). The authors suggested that this third body is formed from mixed, grinded and sintered debris reacting with surrounding oxygen. The glaze layer was found to be stable above 450 °C, which correlated well with the low friction and wear values [21]. The authors also evaluated the wear behavior of pure cobalt, chromium and nickel to identify the distinct roles of Haynes 25 elements and observed the glaze layer formation in cobalt–cobalt contacts leading to lower friction and wear compared to chromium–chromium and nickel–nickel interfaces [20].

Scott et al. [15] attributed the low friction and wear of Stellite 31 at elevated temperatures to the formation of a thermally softened oxide layer (i.e., glaze). In addition, the authors identified that under their sliding conditions the glaze layer formation occurs in the experiments above 523 K and varies with time of sliding. Indeed, the experiments here with the single crystal alloy were performed at much higher temperatures resulting in rapid formation of a protective oxide layer.

The mechanism of friction reduction with the formation of an oxide glaze layer has been previously compared to the Bowden and Tabor concept resulting in low friction and wear [14, 22, 23] in a similar matter as lubricious oxide coatings [24]. According to Bowden and Tabor, the ideal situation for achieving low friction and wear is with a thin and soft coating on top of a hard substrate [23]. Accordingly, in the case of the single crystal evaluated here, thin Co-based oxide layer is formed on top of the Ni-based alloy/Ni oxide region, possibly achieving a similar condition.

4 Conclusion

In this study, the friction and wear behavior of single crystal superalloys were investigated at elevated temperatures. Pin-on-plate experiments were performed on conventionally heat-treated single crystal, coarse γ′ single crystal and Waspaloy® plates using a conventionally heat-treated single crystal for all experiments. In addition, ex situ analysis by means of FIB/SEM and XPS analysis was performed in order to capture the underlying mechanisms leading to the friction and wear behavior of the different alloys. The coefficient of friction for the single crystal materials (i.e., during running-in and steady state) was lower compared to the Waspaloy®. The experiments showed that the friction coefficient of the single crystal is dependent on the crystallographic plane; the friction coefficient was higher for the tests on the {100} plane compared to the {111} plane. The wear behavior was similar to the friction results, where the conventionally heat-treated single crystal showed higher wear resistance compared to the Waspaloy®. However, the coarse γ′ single crystal showed the highest wear, which is attributed to the lower hardness compared to the other alloys tested in this study. Ex situ analysis by means of FIB/SEM and XPS analysis revealed the formation of Co-based metal oxide layer on the surface of the single crystal. Similarly, a Co-based oxide layer is observed on the counterface providing a self-mated oxide-on-oxide contact and thus lower friction and wear compared to the Waspaloy®.

Acknowledgements The authors thank Dr. Agnieszka Wusatowska-Sarnek for the valuable discussions and suggestions on this topic.

References

1. Reed, R.C.: The Superalloys: Fundamentals and Applications. Cambridge University Press, Cambridge (2006)
2. Fecht, H., Furrer, D.: Processing of nickel-base superalloys for turbine engine disc applications. Adv. Eng. Mater. **2**(12), 777–787 (2000)
3. Huda, Z., Edi, P.: Materials selection in design of structures and engines of supersonic aircrafts: a review. Mater. Des. **46**, 552–560 (2013)
4. Meetham, G.W.: High-temperature materials—a general review. J. Mater. Sci. **26**(4), 853–860 (1991)
5. Kozar, R.W., Suzuki, A., Milligan, W.W., Schirra, J.J., Savage, M.F., Pollock, T.M.: Strengthening mechanisms in polycrystalline multimodal nickel-base superalloys. Metall. Mater. Trans. A **40**(7), 1588–1603 (2009)
6. Sims, C.T., Stoloff, N.S., Hagel, W.C.: Superalloys II: High-Temperature Materials for Aerospace and Industrial Power, 2nd edn. Wiley, London (1987)
7. Pollock, T.M., Tin, S.: Nickel-based superalloys for advanced turbine engines: chemistry, microstructure, and properties. J. Propuls. Power **22**(2), 361–374 (2006)
8. Betteridge, W., Shaw, S.W.K.: Development of superalloys. Mater. Sci. Technol. **3**(9), 682–694 (1987)
9. Koizumi, Y., Kobayashi, T., Yokokawa, T., Zhang, J., Osawa, M., Harada, H., Aoki, Y., Arai, M.: Development of next-generation Ni-base single crystal superalloys. Superalloys **2004**, 35–43 (2004)
10. Caron, P., Tasadduq, K.: Evolution of Ni-based superalloys for single crystal gas turbine blade applications. Aerosp. Sci. Technol. **3**(8), 513–523 (1999)
11. Willey, S.A.: The engines of Pratt & Whitney: a technical history. Air Power Hist. **58**(1), 50–52 (2011)
12. Huang, X., Gibson, T.E., Zhang, M., Neu, R.W.: Fretting on the cubic face of a single-crystal Ni-base superalloy. Tribol. Int. **42**, 875–885 (2009)
13. Blau, P.J.: Elevated-temperature tribology of metallic materials. Tribol. Int. **43**, 1203–1208 (2010)
14. Scharf, T.W., Prasad, S.V., Kotula, P.G., Michael, J.R., Robino, C.V.: Elevated temperature tribology of cobalt and tantalum-based alloys. Wear **330–331**, 199–208 (2015)
15. Scott, F.H., Stevenson, C.W., Wood, G.C.: Friction and wear properties of Stellite 31 at temperatures from 293 to 1073 K. Met. Technol. **4**(1), 66–74 (1977)
16. Lawen, J.L., Calabrese, S.J., Dinc, O.S.: Wear resistance of super alloys at elevated temperatures. ASME. J. Tribol. **120**(2), 339–344 (1998)
17. Biesinger, M.C., Payne, B.P., Grosvenor, A.P., Lau, L.W.M., Gerson, A.R., Smart, R.S.C.: Resolving surface chemical states in XPS analysis of first row transition metals, oxides and hydroxides: Cr, Mn, Fe, Co and Ni. Appl. Surf. Sci. **257**, 2717 (2011)
18. Peterson, M.B., Florek, J.J., Lee, R.E.: Sliding characteristics of metals at high temperatures. ASLE Trans. **3**, 101–109 (1960)
19. Viat, A., Bouchet, M.I.D.B., Vacher, B., Le Mogne, T., Fouvry, S., Henne, J.F.: Nanocrystalline glaze layer in ceramic–metallic interface under fretting wear. Surf. Coat. Technol. **308**, 307–315 (2016)
20. Viat, A., Dreano, A., Fouvry, S., Bouchet, M.I.D.B., Henne, J.F.: Fretting wear of pure cobalt chromium and nickel to identify the distinct roles of HS25 alloying elements in high temperature glaze layer formation. Wear **376**, 1043–1054 (2017)
21. Viat, A., Guillonneau, G., Fouvry, S., Kermouche, G., Sao Joao, S., Wehrs, J., Michler, J., Henne, J.F.: Brittle to ductile transition of tribomaterial in relation to wear response at high temperatures. Wear **392**, 60–68 (2017)
22. Scharf, T.W., Prasad, S.V.: Solid lubricants: a review. J. Mater. Sci. **48**, 511–531 (2013)
23. Bowden, F.P., Tabor, D.: The Friction and Lubrication of Solids. Oxford University Press, New York (1950)
24. Aouadi, S.M., Gao, H., Martini, A., Scharf, T.W., Muratore, C.: Lubricious oxide coatings for extreme temperature applications: a review. Surf. Coat. Technol. **257**, 266–277 (2014)